

Article

Provenance of Ordovician Malieziken Group, Southwest Tarim and Its Implication on the Paleo-Position of Tarim Block in East Gondwana

Zhe Chang ^{1,2}, Zhiqian Gao ^{1,2,*}, Liangliang Zhang ³, Tailiang Fan ^{1,2}, Duan Wei ^{1,2} and Jingbin Wang ^{1,2,4}

- ¹ School of Energy Resources, China University of Geosciences, Beijing 100083, China
² Key Laboratory of Marine Reservoir Evolution and Hydrocarbon Enrichment Mechanism, Ministry of Education, China University of Geosciences, Beijing 100083, China
³ State Key Laboratory of Geological Processes and Mineral Resources, Institute of Earth Sciences, China University of Geosciences, Beijing 100083, China
⁴ Petroleum Exploration and Production Research Institute, SINOPEC, Beijing 102206, China
* Correspondence: gzq@cugb.edu.cn

Abstract: Tarim is inferred to have a close connection with East Gondwana during the Ordovician, but the position in East Gondwana remains controversial. In this study, we report 316 detrital zircons U-Pb data from three samples of Ordovician Malieziken Group sedimentary rocks, collected in the Qiate Section, Southwest Tarim, provided new insight into the position of Tarim in East Gondwana. Detrital zircons data indicated the maximum depositional age for the three samples is 489.5 Ma, 478.1 Ma, and 465 Ma, respectively, indicating the Qiate and Kandilike Formation of the Malieziken Group was deposited in Early—Middle Ordovician. The detrital zircons are characterized by two main peaks at ~490 Ma and ~1100 Ma, and three subordinate peaks at ~880 Ma, ~1400 Ma, and ~1650 Ma, suggesting most of the detritus of Malieziken Group from the South Kunlun Terrane (SKT) itself. However, the source of the ~1650 Ma peak is not found in the Tarim block, and the ~1400 Ma and the ~1650 Ma peak are absent in the middle of the three samples, which implied that there is an exotic source. The Paleoproterozoic sediment strata in the Albany–Fraser belt shows dominant peaks at ~1400 Ma and ~1650 Ma may have been transported to SKT and redeposited in the Malieziken Group during the Ordovician. The Malieziken Group shows detrital zircon age patterns resembling those of East Sumatra, Lhasa, and Western Australia which, in combination with the Albany–Fraser belt provenance, enables us to propose that the Tarim block has a close linkage with Western Australia, East Sumatra, and Lhasa in East Gondwana.

Keywords: detrital zircon ages; Malieziken Group; South Kunlun Terrane; Tarim; Gondwana



Citation: Chang, Z.; Gao, Z.; Zhang, L.; Fan, T.; Wei, D.; Wang, J. Provenance of Ordovician Malieziken Group, Southwest Tarim and Its Implication on the Paleo-Position of Tarim Block in East Gondwana. *Minerals* **2023**, *13*, 42. <https://doi.org/10.3390/min13010042>

Academic Editors: Davide Lenaz, Zhenyu Chen and Fangyue Wang

Received: 29 November 2022
Revised: 17 December 2022
Accepted: 19 December 2022
Published: 27 December 2022



Copyright: © 2022 by the authors. Licensee MDPI, Basel, Switzerland. This article is an open access article distributed under the terms and conditions of the Creative Commons Attribution (CC BY) license (<https://creativecommons.org/licenses/by/4.0/>).

1. Introduction

The configuration of the major crustal blocks (e.g., India, Australia, East Antarctica, and Africa) that constitute the core of the Gondwana have been well constrained [1–3]. During the Ordovician, Asian blocks (such as South China, North China, Tarim, Lhasa, and Sibumasu) were located in the northeastern peri-Gondwana region [4–7]. However, the exact positions of Tarim in northeastern Gondwana are still controversial. The position of the Tarim in Gondwana is crucial for understanding its evolution.

Some authors suggested that the Tarim block was an isolated block [3], whereas other models considered the Tarim block was welded into the north margin of East Gondwana, following the consumption and closure of the Proto-Tethys Ocean [3,8,9]. To date, some studies proposed the position of the Tarim block was adjacent to Iran–Saudi Arabia during the Early Paleozoic [9–12]. Several studies have inferred a close affinity between Tarim and North India, based on provenance investigation into Neoproterozoic to Early Paleozoic strata in South Tarim [10–12]. A long-held hypothesis suggests a close connection between

Tarim and Australia in Gondwana [13–16]. Recently, Fang et al. (2019) [7] suggest a South China–Tarim–Tibet–Sibumasu biogeographic province during the Late Ordovician, based on the cephalopods in these blocks.

Most researchers favor the notion that the close of the Proto-Tethys Ocean during the Early Paleozoic caused the South Kunlun Terrane (SKT) to amalgamate to the North Kunlun Terrane (NKT), which is regarded as part of the South Tarim Terrane (STT), with the remnants of the Proto-Tethys Ocean preserved along the Oytag–Kudi suture zone [17–19]. The South Kunlun Terrane (SKT) exposes Early Paleozoic igneous and sedimentary rocks, particularly the Malieziken Group, which is composed of marine clastic and carbonate rocks. There are several previous studies which constrained the depositional age of the Malieziken Group to the Early [20], Middle [21,22], or Late [23,24] Ordovician, but the provenance of the Malieziken Group is poorly investigated. The provenance analysis of the Malieziken Group is significant for the problem of Tarim tectonic position relative to adjacent blocks.

Detrital zircons U-Pb data from sedimentary rocks can be used to constrain the maximum depositional age (e.g., [25,26]), provenance and the affinities of terranes [12,27–29]. Certain age components may be particularly significant as an indicator of a specific provenance [30]. In this study, we carried out U-Pb isotopic analysis on detrital zircons from the Ordovician Malieziken Group, collected from the Qiate section, southwestern Tarim, in combination with previously published data, to reveal the possible position of Tarim. Our conclusion shows that the Tarim is close to Western Australia, Lhasa, and East Sumatra in northeastern Gondwana during the Ordovician.

2. Geological Background

2.1. Tectonic Setting

The Tarim Basin is a cratonic basin in northwestern China, bounded by Tianshan Mountain to the north, Kunlun Mountain to the southwest, and Altyn Mountain to the southeast, respectively, covering an area of about 56×10^4 km² (Figure 1a). The Precambrian basement is mainly composed of Archean to Early Neoproterozoic metamorphosed strata and igneous rocks, which are exposed in marginal uplifts of the block (the Aksu, Tiekelike, Quruqtagh, and the Altyn areas) and are identified in central Tarim drill core. Neoproterozoic–Cenozoic strata unconformably overlie the Precambrian basement [19,31,32]. The Tarim block is composed of two distinct terranes, the North Tarim Terrane (NTT) and the South Tarim Terrane (STT). Previous studies have shown that the NTT amalgamated with the STT before ca. 820 Ma along the central Tarim suture zone (CTSZ) (before Nanhuanian) [33–35]. The STT geological evolution is poorly investigated because of difficult access.

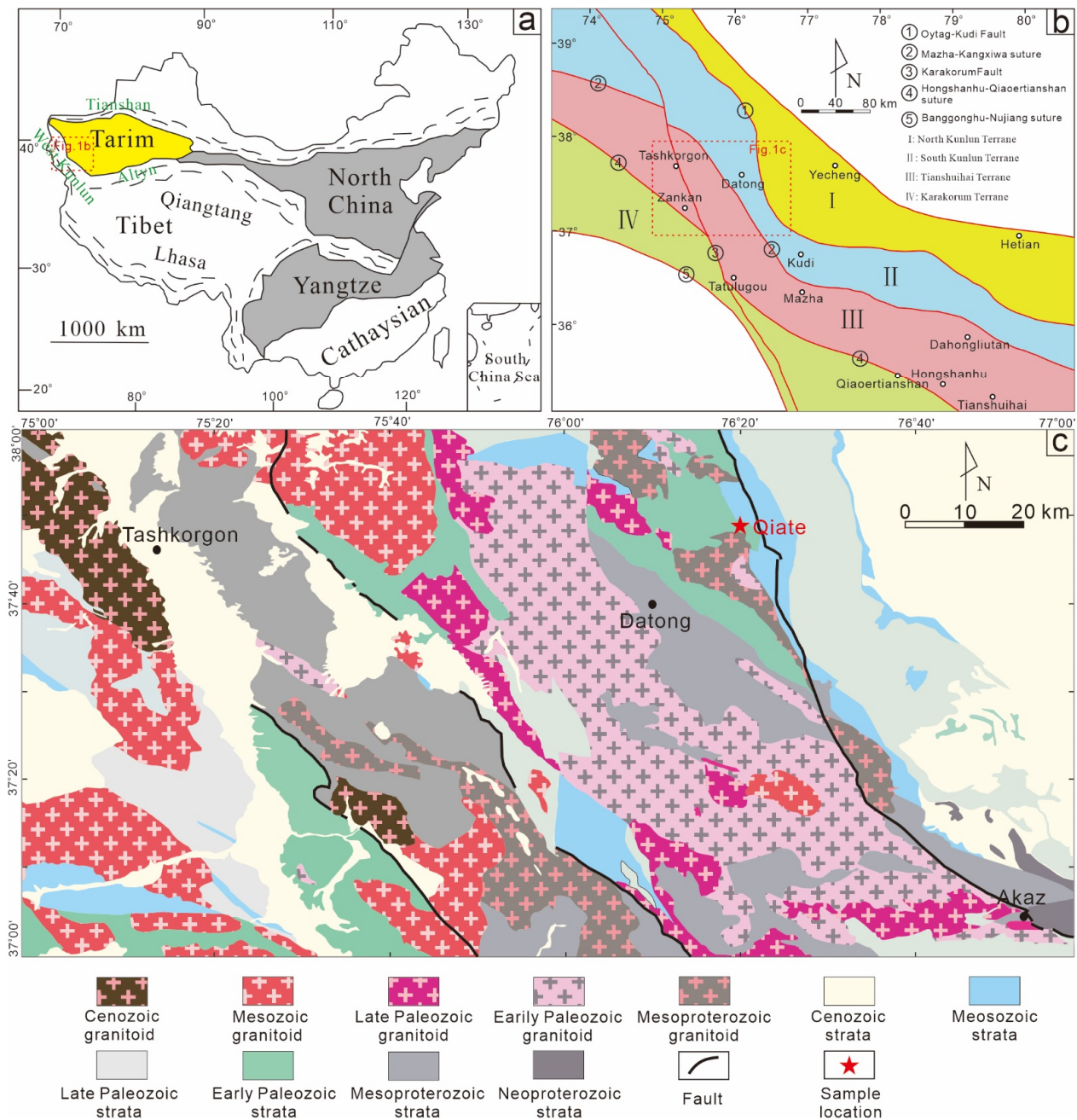


Figure 1. (a) Tectonic subdivision of China showing the location of the Tarim block, North Tarim Terrane, and South Tarim Terrane modified from [34]; (b) Tectonic subdivision of west Kunlun orogenic belt (modified from [36]); (c) Simplified geologic map of the central-west part of the West Kunlun orogenic belt (after [37]), showing the location of the Qiate section.

The west Kunlun orogenic belt (WKO) is subdivided into four main units: the North Kunlun Terrane (NKT), the South Kunlun Terrane (SKT), the Tianshuihai Terrane (TSHT), and Karakorum Terrane (KAT), are bound by the Oyttag–Kudi fault, Mazar–Kangxiwar suture Hongshanhu–Qiaortianshan suture, and Bangonghu–Nujiang suture, respectively (Figure 1b, [17,18,36,38–41]). The WKO evolution was closely related to the subduction of the Proto- and Paleo-Tethys Ocean [17,42–44]. Multiphase tectonothermal events were recorded by the Precambrian to Cenozoic sedimentary rocks, igneous rocks, and metamorphic rocks [28,45,46].

The NKT is regarded as part of the southwestern margin of the STT and has recorded tectonic evolution from Early Paleoproterozoic to Early Paleozoic [19,20]. The NKT Paleo-

Neoproterozoic basement consists of Heluositan granitic complex, Ailiankate Groups, and Sailajiazitage Groups [19,47–49]. During the Mesoproterozoic to mid-Neoproterozoic, the NKT was mainly composed of metamorphosed strata and diverse igneous rocks. Late-Neoproterozoic is characterized by a carbonate–clastic–tillite sequence. The Mesoproterozoic to Neoproterozoic strata can be related to the evolution of the Rodinia supercontinent. The assembly of Tarim and the Rodinia supercontinent was recorded by the Klakashi Group metamorphic rocks (ca. 1000 Ma) [19].

The SKT basement is composed of a Mesoproterozoic to Neoproterozoic metamorphic complex, which is mainly consisted of schist and gneiss locally intercalated with ultramafic lenses [50,51]. The SKT was an exotic block accreted to the North Kunlun Terrane during the Early Paleozoic [39,43,52]. The outcropped Precambrian basement in the SKT is comprised of the Pushou Group and the Sangzhutage Group in the north and the Saitula Group in the south, separated by the Pushou–Menggubao ophiolitic mélangé [53].

The Oyttag–Kudi–Qimanyute (OKQ) suture zone is the boundary between the NKT and SKT [54–56]. The OKQ comprises an alignment of ophiolite suites (e.g., the Kudi ophiolite and the Qimanyute ophiolite) [57], and is regarded to be a remnant of the Proto-Tethys Ocean [17,18]. During the Cambrian to the Ordovician (530–466 Ma) the OKQ developed a back-arc basin with bidirectional subduction (mainly southward subduction); During the Late Middle Ordovician–middle Late Ordovician (460–450 Ma), the NKT and the SKT collision took place, which causes the termination of marine sedimentation and minor syn-collisional peraluminous magmatism; The middle Late Ordovician–Late Silurian (450–428 Ma) was the collisional orogenic stage. The closure time of the Proto-Tethys Ocean and the related collision took place during the Late Ordovician–Middle Silurian in West Kunlun Orogen [19,58,59].

2.2. Field Observation

During the Neoproterozoic to Cambrian, the STT evolved from fault-depression basins into passive continental margins [60]. The Tarim basin developed a carbonate platform from Cambrian to Middle Ordovician [61].

This study mainly focuses on the Ordovician Malieziken Group exposed in the north margin of SKT (Figure 1). The Malieziken Group was named by the Ministry of Geology in 1958, being exposed near the Malieziken Mountain (such as the Qiate section), Shache County, subdivided into four formations from bottom to top: the Qiate formation, the Kandilike Formation, the Botazi Formation, and the Kuweixi Formation. This Group is characterized by clastic–carbonate sedimentary rocks with abundant bioclastic or fossils. The top of the Malieziken Group is not cropped. The bottom of the Malieziken Group is in contact with the underlying Mesoproterozoic Sangzhutage group and intrusion rocks by unconformities (Figures 1c and 2, [20,24,62]). The Malieziken Group may deposit during the Early [20], Middle [21,22], or Late [23,24] Ordovician.

The Qiate Formation (Figures 3D–I and 4D–I) is mainly composed of a conglomerate in the lower part with interbedded fine-grained quartz sandstone, the grain size decreases upward. The depositional environment of the Qiate Formation was shoreface. Clasts in the conglomerate are well-rounded but poorly sorted, mostly grain-supported. The gravel ranges from 1–10 cm in size, and the components of which are dominated by quartzite, chert, and vein quartz. Horizontal bedding, rhythmic bedding, and wedge-shaped cross stratification have been identified, suggesting a shoreface environment.

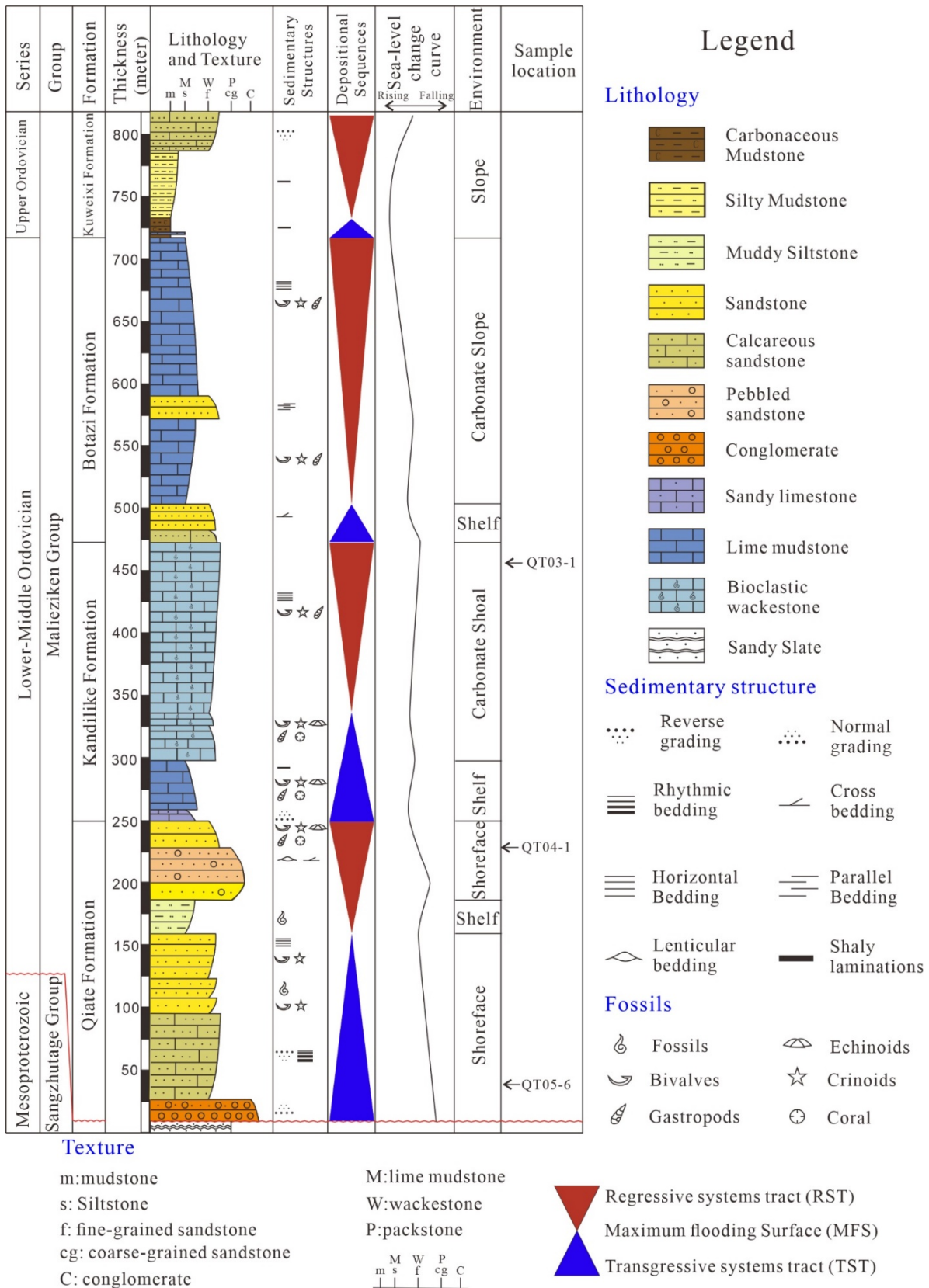


Figure 2. Sedimentary column showing lithological packages and sedimentary evolution of the Malieziken Group in Qiate Section, showing the three sample locations (modified from [62]).



Figure 3. (A): The start point of the Qiate Section; (B): QT03-1, Grey-black thinly laminated bioclastic lime mudstone; (C): QT03-1, Algal of the lime mudstone; (D): Near QT04-1, the diabase intrusion; (E): QT04-1, greyish green conglomerate sandstone interbedded with coarse grained quartz; (F): Brachiopods in the bioclastic calcareous quartz sandstone in Qiate Formation; (G): Grey thick bedded fine grained quartz sandstone interbedded with grey thinly laminated bioclastic calcareous fine grained quartz sandstone. Bed thicknesses increase upward; (H): QT05-6, Grey, thick bedded, calcareous quartz sandstone; (I): unconformable contact between the Ordovician Malieziken Group and Mesoproterozoic Sangzhutage Group.

The Kandilike Formation (Figures 3A–C and 4A–C) is characterized by bioclastic limestone that contains abundant fossils of crinoid stems, bivalves, and gastropods, implying a shallow marine carbonate platform setting. Lime mudstone to packstone and horizontal bedding combined with the fossils indicates a carbonate shoal depositional environment.

The Botazi Formation is dominated by mud limestone with parallel bedding, the grain size and thickness of the beds decrease upward. Bioclastic mainly includes crinoid stems, bivalves, and gastropods, the proportion of which is about 10% and reduce upward. The depositional environment of the Botazi Formation is a carbonate slope.

The lower part of the Kuweixi Formation is characterized by grey-black carbonaceous mudstone with shaly laminations, whereas the upper part of this formation is mainly grey silty lime mudstone with interbedded light grey calcareous, fine-grained quartz sandstone.

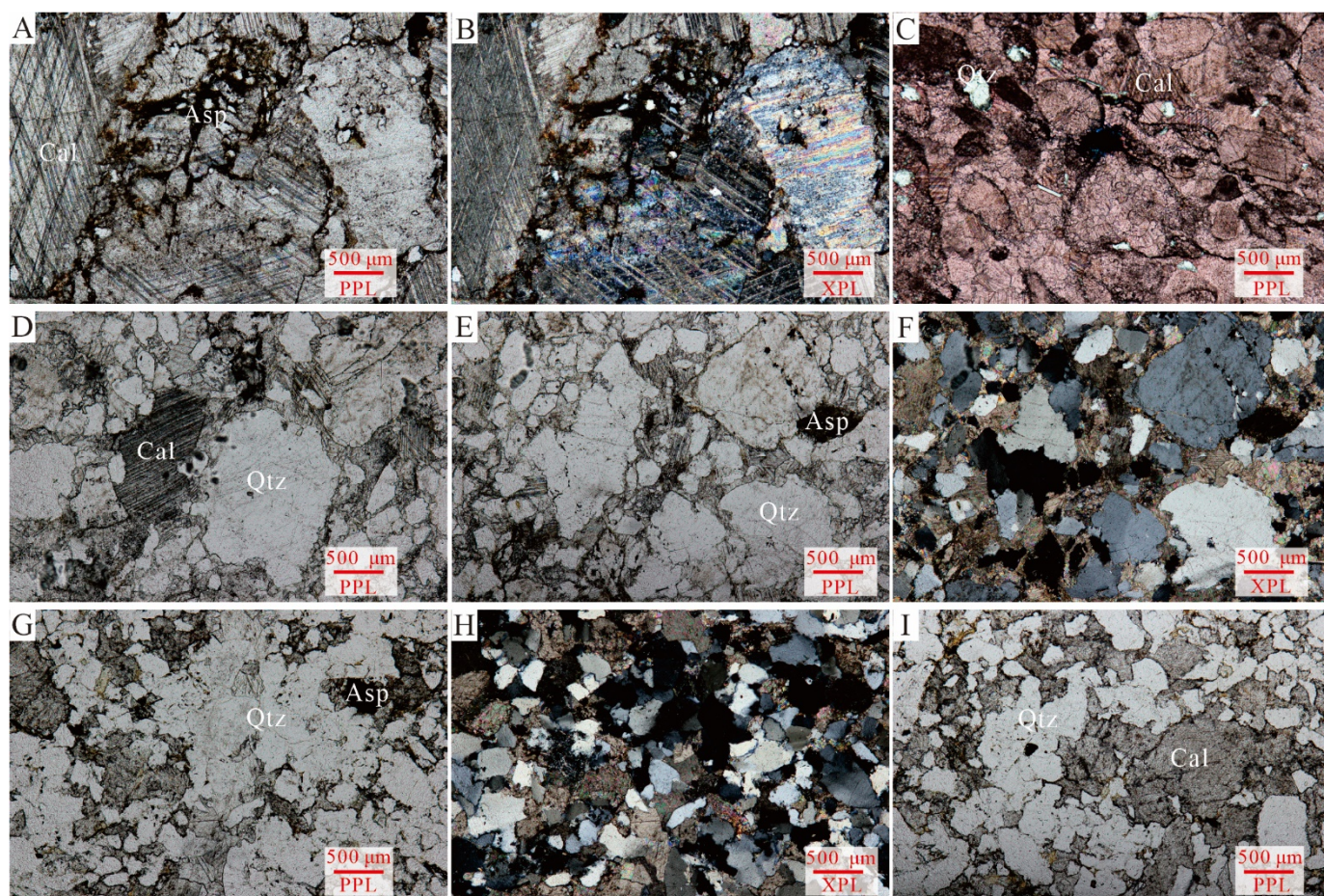


Figure 4. (A–C), QT03-1, grey-black mud limestone or algal limestone, with Ostracode and peloids; (D–F), coarse-grained sandstone, the matrix is clay mineral and calcareous cementation; (G–I), fine-grained calcareous sandstone, calcareous cementation. PPL: plane-polarized light; XPL: cross-polarized light; Qtz: Quartz; Cal: Calcite; Asp: Asphalt.

3. Sampling and Analytic Methods

3.1. Sample Descriptions

We conducted detrital zircon U-Pb age isotopic analysis on three samples collected from the Qiate Section (Qiate Village: GPS: 37°48'04" N; 76°21'13" E; 2876 m) in the north margin of SKT. The geographic location of the Qiate section is given in the geological map (Figure 1c), and the stratigraphic location of the three samples is given in the stratigraphic columns (Figure 2).

The sample QT03-1 (GPS: 37°48'19" N; 76°20'35" E; 3085 m) was collected from the top of the Kandilike formation. It is a grey-black mud limestone or algal limestone (Figure 3B,C). The mineral is dominated by ~70% of calcite with a small proportion of terrigenous detrital minerals such as quartz (Figure 4A–C).

The sample QT04-1 (GPS: 37°48'18" N; 76°20'37" E; 3019 m) is a coarse-grained sandstone (Figure 3D–F) obtained from the uppermost area of the Qiate Formation. It contains ~70% of quartz and ~10% of Calcite, and the matrix is clay mineral and calcareous cementation (Figure 4D–F).

The sample QT05-6 (GPS: 37°48'11" N; 76°20'52" E; 3019 m) is a fine-grained calcareous sandstone (Figure 3G–I) obtained from the lower part of the Qiate Formation. It contains ~50% of quartz and ~20% of calcites, the matrix is clay mineral and calcareous cementation (Figure 4G–I).

3.2. Zircon LA-ICP-MS Analysis

Zircons were separated from the crushed samples by heavy-liquid and magnetic methods. Individual grains were handpicked under a binocular microscope, mounted in epoxy resins and then polished to expose the grain centers. Cathodoluminescence (CL) images were obtained using an electron microprobe for choosing the analysis sites within the zircons. LA-ICP-MS U-Pb isotope and trace elements of zircons were measured at the Milma Lab of China University of Geosciences (Beijing) by using an Agilent 7900 ICP-MS system attached to a NewWave 193^UC excimer laser ablation system. The carrier gas transported the ablated material to the plasma source of an Agilent 7900 ICP-MS. We used the 33 μm laser beam diameter with the laser energy of 3 J/cm² and a frequency of 8 Hz. The details of this procedure were described in [63].

Zircon 91500 and NIST SRM 610 synthetic glass were used as external standards for correcting mass discrimination and elemental fractionation for U-Pb dating and trace element analysis. The 91500 was analyzed twice every 15–20 analysis of zircon samples and the NIST SRM 610 was analyzed once every 30–40 zircon samples. Zircon standards GJ-1 were analyzed as unknown samples that were inserted between 91500 and the samples. We obtained a weighted mean ²⁰⁶Pb/²³⁸U age of 600.9 ± 1.1 Ma (2SD, *n* = 20) for GJ-1 which is consistent with recommended values within the error of recommended values [63,64].

Ages with concordance lower than 90% were excluded. The ²⁰⁶Pb/²³⁸U age is used when the ²⁰⁶Pb/²³⁸U age is younger than 1000 Ma, otherwise the ²⁰⁷Pb/²⁰⁶Pb age is used [65]. U-Pb concordia diagrams, histograms, and probability density plots were made by Isoplot [66].

4. Results

Three Ordovician samples of the Qiate Section were collected for zircon U-Pb dating (Figures 1c and 2), and a total of 316 detrital zircon grains were analyzed. Representative cathodoluminescence (CL) images of zircons and corresponding ²⁰⁷Pb/²⁰⁶Pb ages (>1000 Ma), ²⁰⁶Pb/²³⁸U ages (<1000 Ma) shown in Figure 5. Zircons from QT05-6 are coarser (>100 μm in length) than those from QT03-1 and QT04-1 (<100 μm in length). Most of the zircons have width/length ratios of 1:1.5–1:2 and are rounded to subrounded in shape. Narrow oscillatory zone is visible under CL, some grains show bright or dark overgrowth rims or core-rim structures that indicated a later metamorphic overprint, and some grains exhibit homogenous internal structures. The Th/U ratio is regarded as an indicator to distinguish magmatic zircons (>0.4) from metamorphic zircons (<0.1) [67]. About 46% of these zircons exhibited high Th/U (>0.4), which represented igneous detrital zircons, and about 17% of them exhibited low Th/U (<0.1), which represented metamorphic zircons (Figure 6). There are more metamorphic zircons in grains with younger age. This implies the source of detritus from metamorphic rocks.

Each sample (about 5 kg) included over 1000 zircon grains, we analyzed 90–120 grains for each sample. Zircons U-Pb concordia diagrams, histograms, and probability curves are shown in Figure 7. A total of 112 zircons from QT03-1 yield one prominent age population at 1138 Ma, and four subordinate age peaks at 500 Ma, 889 Ma, 1411 Ma, and 1660 Ma. A total of 93 zircons from QT04-1 display one prominent age at 1086 Ma, and two subordinate ages at 490 Ma and 894 Ma, age peaks at ~1410 Ma and ~1660 Ma are not detected. A total of 111 zircons from QT05-6 exhibit one prominent age population at 1379 Ma, and two subordinate age peaks at 1145 Ma and 1654 Ma. The cumulative proportion of the detrital zircon is shown in Figure 8, indicating the tectonic setting of the Malieziken Group was a collisional setting [68].

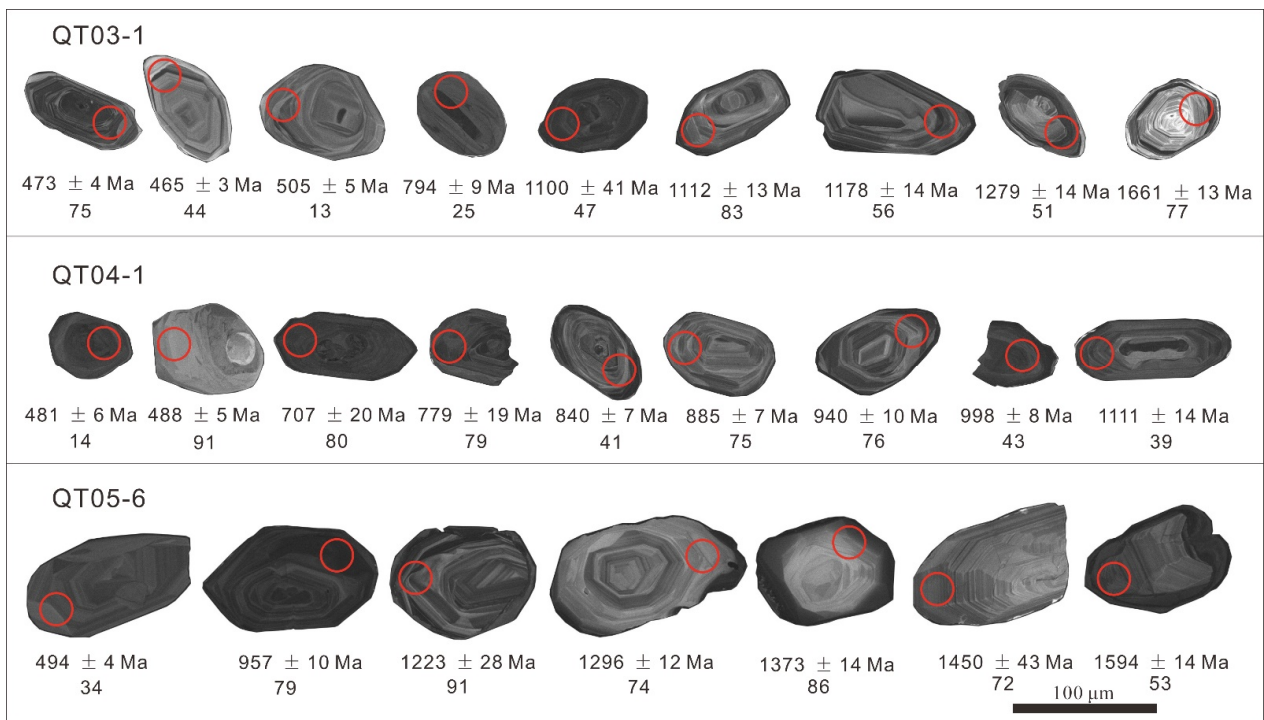


Figure 5. Representative cathodoluminescence images of zircons and corresponding $^{207}\text{Pb}/^{206}\text{Pb}$ ages (>1000 Ma), $^{206}\text{Pb}/^{238}\text{U}$ ages (<1000 Ma) values.

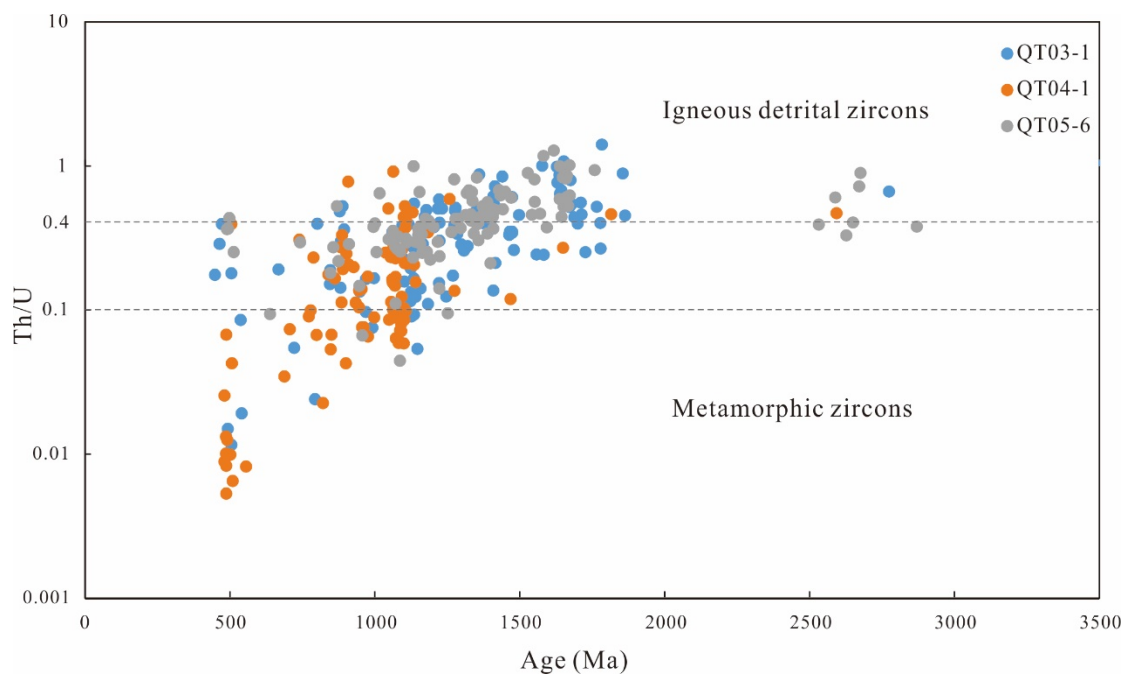


Figure 6. Age vs. Th/U ratio diagrams, magmatic zircons with >0.4 and metamorphic zircons <0.1 [67].

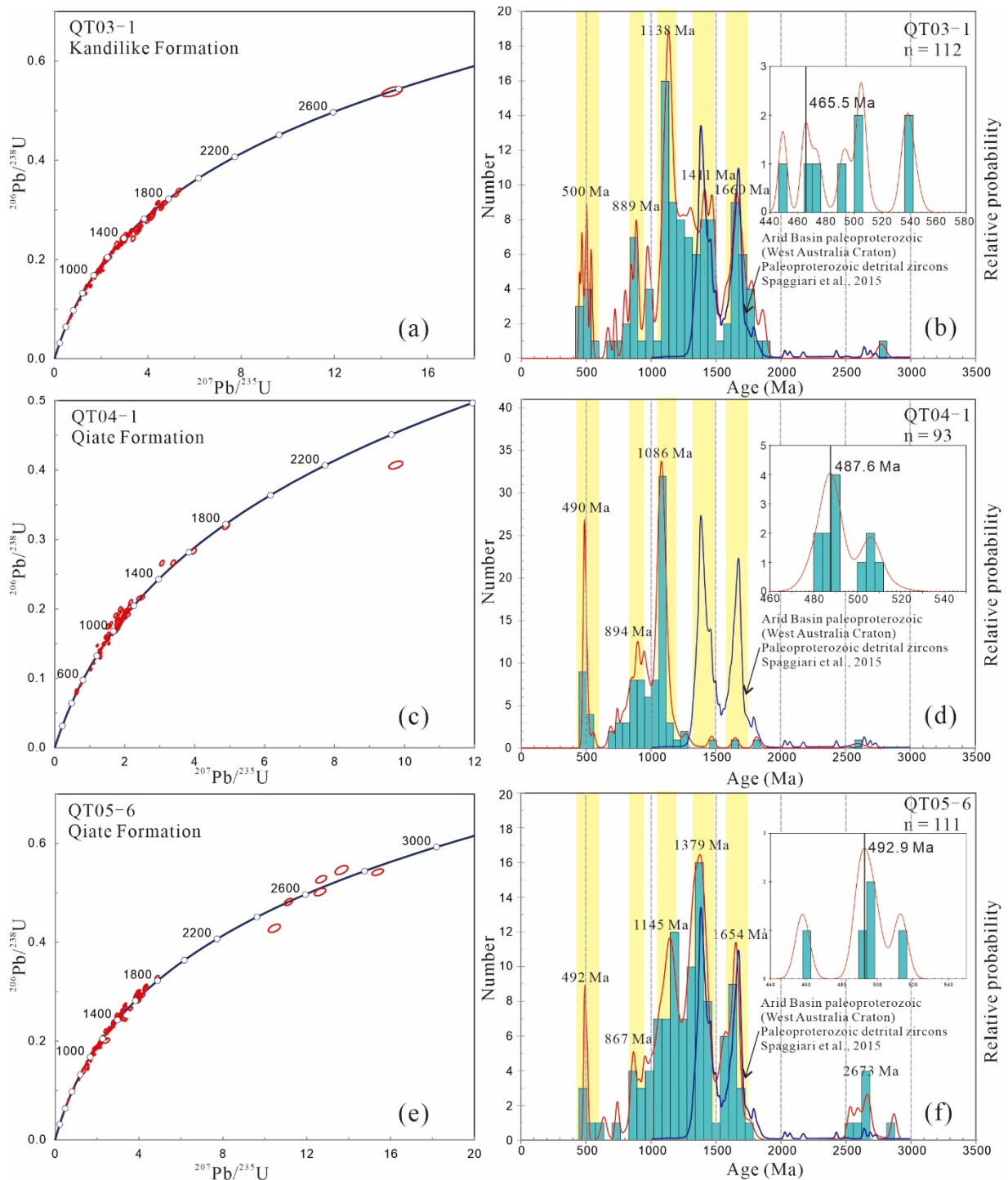


Figure 7. U–Pb Concordia diagrams (a,c,e) and age spectra (b,d,f) for zircons from the Malieziken Group. The ellipse shows a 2-sigma error. N represents the number of analyzed zircon grains. YPP age is shown on the right side. The blue curve shows probably the source of ~1400 Ma and ~1650 Ma zircons from Western Australia [69].

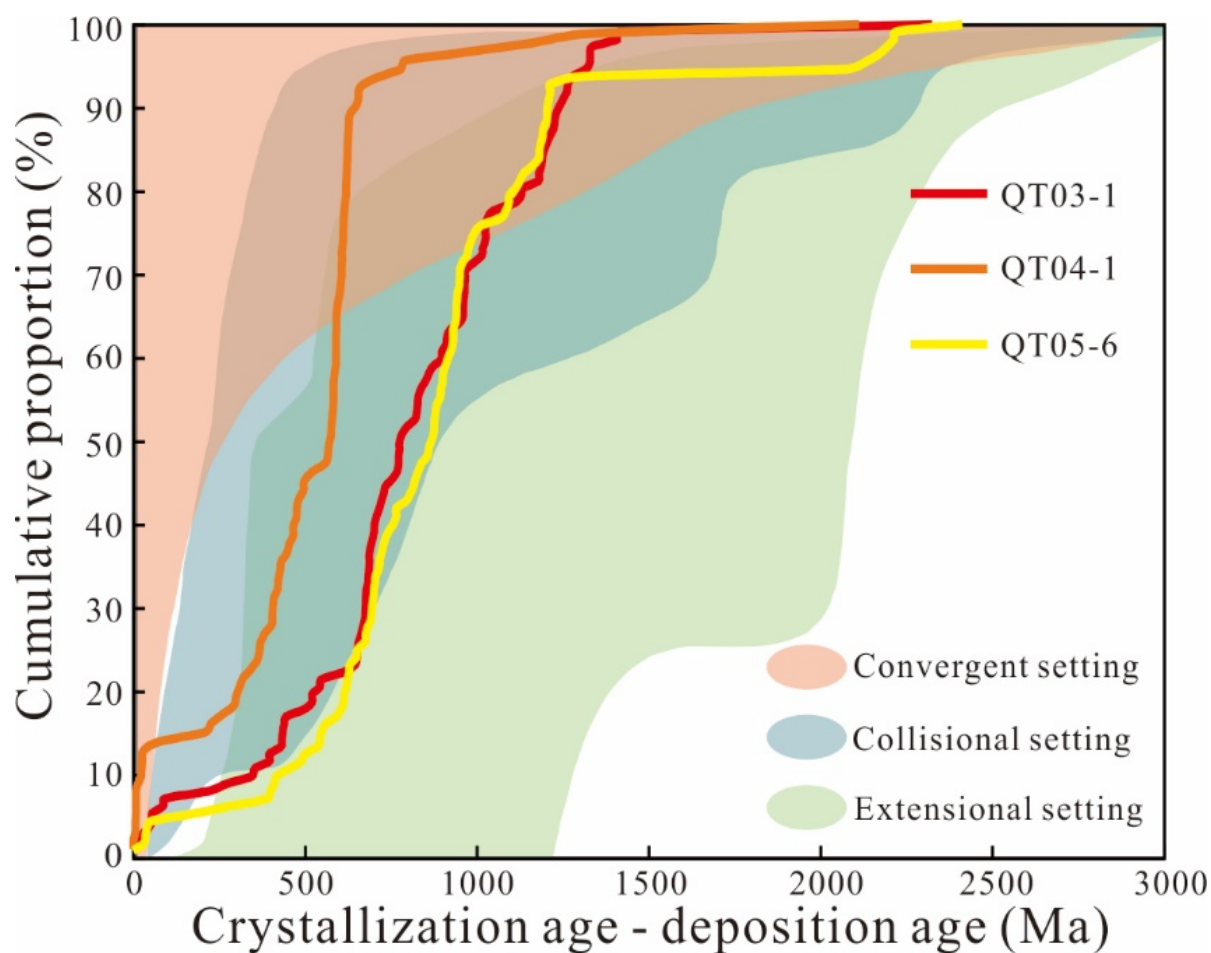


Figure 8. Cumulative proportion of the detrital zircon U-Pb ages plot showing the tectonic setting of the Malieziken Group, modified from [68].

All the zircons exhibit five age clusters that are comparable with adjacent continent (Figure 9): (1) ~490 Ma, ca. 480–500 Ma, (Weighted mean age of 489 ± 2.6 Ma, MSWD = 0.95, $n = 12$) (2) ~880 Ma, ca. 850–900 Ma, (Weighted mean age of 880 ± 4.2 Ma MSWD = 2.8 $n = 15$) (3) ~1100 Ma, ca. 1000–1160 Ma, (Weighted mean age of 1097.4 ± 3.2 Ma, MSWD = 5.4, $n = 86$); (4) ~1400 Ma, ca. 1360–1440 Ma, (Weighted mean age of 1401.1 ± 5.4 Ma, MSWD = 2.1, $n = 29$) (5) ~1650 Ma, ca. 1630–1680 Ma, (Weighted mean age of 1654 ± 5.7 Ma, MSWD = 1.12, $n = 21$).

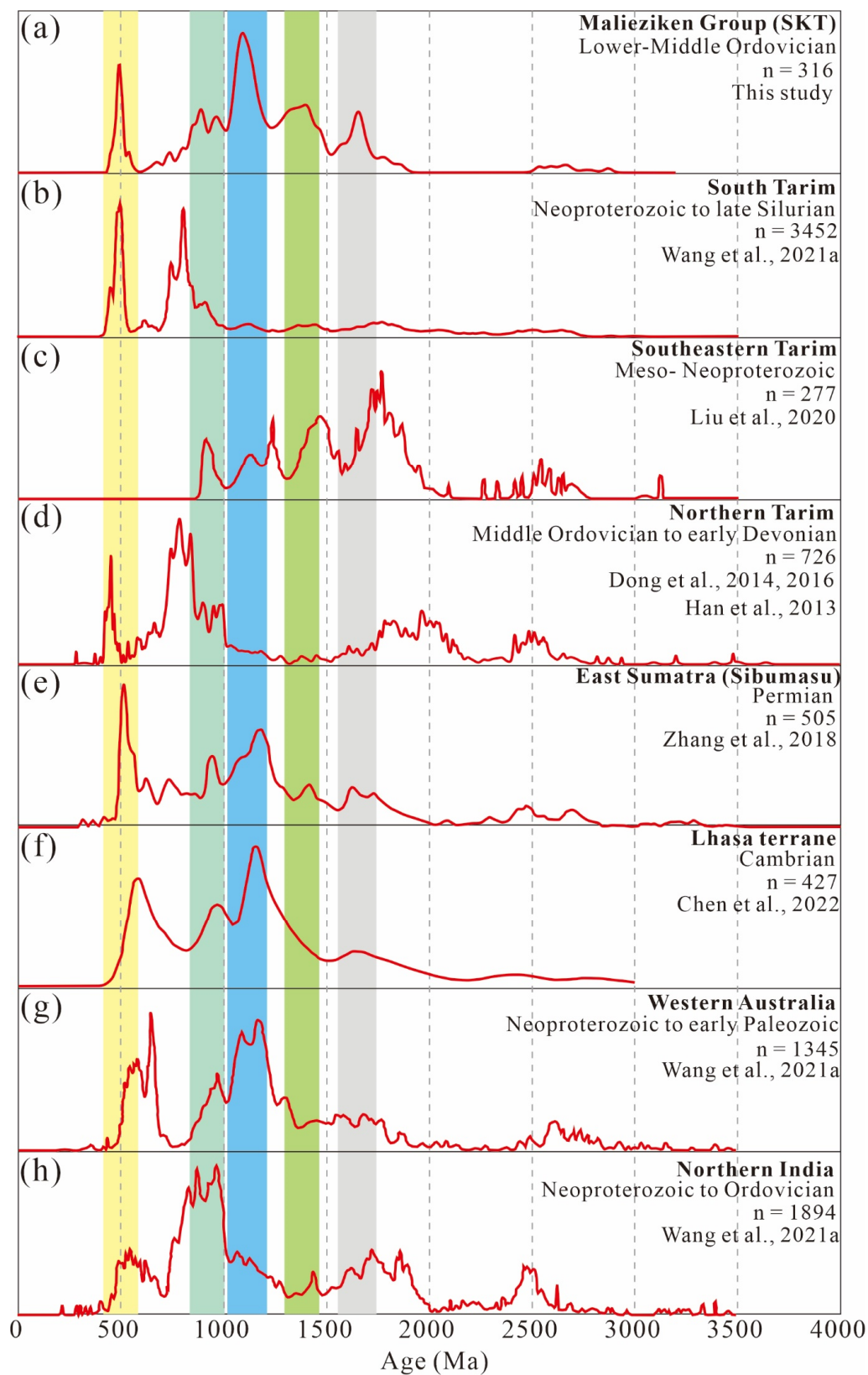


Figure 9. Relative probability diagrams showing the U-Pb age distributions of (a) the Malieziken Group (this study), (b) South Tarim [12], (c) Southeastern Tarim [10], (d) Northern Tarim [28,70,71] and other relevant Rodinia continental blocks, such as (e) Sibumasu [72], (f) Lhasa terrane [73], (g) Western Australia [12], (h) Northern India [12].

5. Discussion

5.1. Maximum Depositional Age

Former studies have reported the biostratigraphic evidence focus on the age of Malieziken Group. In the lower part of the Malieziken Group, the cephalopods *Wutinoceras-Armenoceras* were discovered in the Qiate Section, which is regarded as the Tremadocian (early Early Ordovician) fauna [20]. The *Batostoma jinhongshanense* and *B. altunshanense* was also discovered, which were Late Tremadocian in age (middle Early Ordovician) [22]. In the middle part of the Malieziken Group (limestone of Kandilieke Formation), were found the brachiopods *Anchigonites intermedia*, *Gonambonites? facioostellatus*, *Apatomorpha* sp., *Platymena* cf. *plana*, *Maakina* sp., which were regarded as Middle Ordovician (correlated with Llandeilan in Europe) [21]. The graptolites *Glyptograptus teretiusculus* and *Dicranograptus nicholsoni* from in Calcareous siltstone Kuweixi Formation were interpreted as early Late Ordovician (Sandbian) [23].

It is generally regarded that the youngest zircon age of sedimentary strata is older than the depositional age, therefore, the detrital zircon age can be used to constrain the maximum age of sedimentary strata (e.g., [25,26]).

Direct isotope age data of the Malieziken Group are rare. Qian et al., 2018 proposed the Malieziken Group deposited during the Late Ordovician, based on the youngest detrital zircon age of the Qiate Formation is 459 ± 9 Ma, and the youngest detrital zircon age of the Kandilike Formation is 465.9 ± 9.1 Ma. However, the second youngest grain age of the Qiate Formation in his study is 477.2 ± 9.2 Ma, which does not overlap with the youngest single grain age within 1σ . In addition, the weighted mean age of the 22 youngest grains from the Kandilike Formation is 482.3 ± 5.5 (MSWD = 1.8). The youngest single grain age is not reliable because of the absence of reproducibility and it might be influenced by lead loss [25].

Dickinson and Gehrels (2009) [25] proposed five metrics to determine the maximum depositional age of strata: (1) YSG (youngest single grain age); (2) YPP (youngest graphic age peak); (3) YC1 σ (2+) (youngest 1σ grain cluster); (4) YC2 σ (3+) (youngest 2σ grain cluster); (5) YDZ (age calculated by the “youngest detrital zircon” routine of Isoplot, [66]). Table 1 has contrasted the five metrics of the three samples to determine the maximum age. The youngest single age of QT03-1 and QT05-6 was excluded when calculating the YDZ age, due to the possibility of this age being influenced by possible lead loss, and is spurious (the youngest single age and the second youngest age did not overlap at 2σ , see Table S1). The YPP and the YC1 σ (2+) age may be insensitive for the interpretation of the maximum youngest depositional age [26]. The YC2 σ (3+) is the most conservative measure of youngest age, and it is the least likely of the youngest-age measures to approximate depositional age [25]. YDZ age is accepted in this study as the maximum of the depositional age.

The two YDZ age from the bottom and top of the Qiate Formation is 489.5 Ma and 478.1 Ma, and the YDZ age from the top of the Kandilike Formation is 465 Ma. The diabase dikes intruded into Qiate Formation (Figure 3D). He et al. (2007) [74] reported this diabase intrusion has not intruded into the Silurian in the seismic section, implying the Qiate Formation deposited earlier than Silurian. Combined with the paleontology studies in the Malieziken Group, this study proposes the Qiate Formation was deposited during the Early Ordovician and the Kandilike Formation was deposited during the Early–Middle Ordovician.

Table 1. Ages calculated by five measures of youngest age (See [25]). The youngest single age was excluded when calculating YPP and YDZ age.

Analysis		Samples		
		QT03-1	QT04-1	QT05-6
YSG	Age $\pm 1\sigma$	449 \pm 3	481 \pm 5	458 \pm 4
YPP (see Figure 8)	Age	465.5	487.6	492.9
YDZ	Age	465	478.1	489.5
	Range	+6.2/−6.8	+6.6/−11	+6.6/−9
	Confidence	95%	95%	95%
YC1 σ (2+)	Age	467.9 \pm 4.8 (1.1%)	484.6 \pm 4.8 (1.0%)	493 \pm 5.3 (1.1%)
	Systematic Error	1.1%	1.1%	1.1%
	MSWD	2.6	0.49	0.79
YC2 σ (3+)	Age	501 \pm 17 (0.86%)	487 \pm 3.2 (0.65)	493 \pm 5.3 (1.1%)
	Systematic Error	1.1%	1.1%	1.1%
	MSWD	3.2	0.99	0.79
Accepted age (Ma)		465	478.12	489.58

5.2. Provenance of the Malieziken Group

The zircons in the Malieziken Group are rounded or subrounded in shape, suggesting a long distance from the provenance to the Malieziken Group. However, the conglomerate and sandstone from Qiate Formation are poorly sorted, suggesting a closer source such as the surrounding mountains. Therefore, recycled detrital material might have fed the Malieziken Group.

Figure 8 shows the youngest 5% zircons age “CA – DA < 150” and the youngest 30% zircons age “CA – DA > 100” (CA = crystallization age; DA = depositional age, [68]), implying the tectonic setting of the Malieziken Group is a collision environment. The collision environment is also consistent with the former study of tectonic evolution of WKO, that the NKT and SKT collision along the Oyttag–Kudi–Qimanyute suture (see Section 2.1).

The overall age profile of Malieziken Group samples yields a broad distribution of 450–2800 Ma and displays two predominant early Paleozoic clusters peaking at ~490 Ma and Mesoproterozoic at ~1100 Ma, with minor ages defining subsidiary peaks at ~880 Ma, ~1400 Ma and ~1650 Ma (Figure 9a).

The youngest detrital zircon age population of ca. 480–500 Ma (peak at 491 Ma) correlates well with Early Paleozoic igneous and metamorphic rocks of a similar age in the West Kunlun orogenic belt, which recorded the double-sided subduction of the Proto-Tethys Ocean [35,58,75]. The age of the Kudi ophiolite is demonstrated formed at 525–490 Ma [43,76]. The southward subduction of the Proto-Tethys Ocean during 530–430 Ma [37,42,43]. Felsic lava from the Aqingyan Group in NKT is regarded as the product of the northward subduction of the Proto-Tethys Ocean (487 \pm 7 Ma, [12]). It could be argued that andesite and rhyolite rock (~490 Ma) found in the Altyn mountains [77] could also be a potential source of the youngest detrital zircon population. Moreover, the relative probability diagrams of South Tarim, North Tarim, and East Sumatra detrital zircons also show a major peak at ~490 Ma (Figure 9). In short, this age population is mainly from related metamorphic rocks that result from the subduction of the Proto-Tethys Ocean.

The detrital zircon population of 850–900 Ma (peak at ~880 Ma) was derived from the interior of the Tarim carton. This age population coincides with two orogenic events in the Tarim block: (1) The Early Neoproterozoic Sailajiazitage volcanic rocks (920–870 Ma, also called Sailajiazitage Large Igneous Province) have been identified in the Tiekelik Belt, southeastern part of the Tarim block, which is considered to correlate to the rift-related magmatism in North China, West African, Congo and São Francisco blocks [78]. This event might relate to the plume or superplume that reduced the initial breakup of Rodinia [79]. (2) The amalgamation of the NTT and STT along the central Tarim suture zone between

870 and 820 Ma is demonstrated by the north Altyn suture, drilling core in Central Tarim and paleomagnetic evidence [33–35,80]. However, the age of 870–820 Ma detrital zircons that represent the amalgamation of the NTT and STT event is not remarkable in the south Tarim and North Tarim detrital zircon age spectra (Figure 9b–d), suggesting that this event is not the major source of this age. This detrital zircon age population is also detected in southeastern Tarim and other Gondwana blocks (Figure 9).

The detrital zircon population of 1000–1200 Ma (peak at ~1100 Ma) is the predominant peak of the Malieziken Group, which might be derived from both interior and exterior of the Tarim block. The underlying Sangzhotage Group was emplaced by the granodiorite–augen granite–leucogranite complex emplaced at ca. 1117 Ma, which is the potential source of this age population [41].

The Malieziken Group also detected the age population of 1360–1440 Ma (peak at ~1400 Ma). The ~1400 Ma Azibailedi granitic pluton was reported in SKT, intruding the underlying Sangzhotage group metamorphic strata which were likely deposited during the 1500–1400 Ma is potential source of this age population [49,79].

Yet no corresponding magmatic event or metamorphic event for the ~1650 Ma cluster has been identified in the Tarim block or WKO, implying a second provenance in the Malieziken Group. There are two possibilities for the source of this age population: (1) this age population are redeposited from older sandstones or from a not-identified crustal fragment within the SKT which might have disappeared due to the subduction absorption and/or surface erosion over the last 450 Ma, which implies the SKT underwent a ~1650 Ma event; (2) this detrital material, presumably derived from an exotic source, could be transported over long distances and deposited in the SKT. In Figure 8, samples from QT04-1 at the top of the Qiate Formation fall into a different field. The absence of the two clusters with the peak at ~1400 Ma and ~1650 in the QT04-1 suggests a provenance change during the Malieziken Group deposit. Nearly identical age patterns of the QT04-1 absent age population have been documented from the Paleoproterozoic strata from the Arid basin, Albany–Fraser Orogen (Figure 7, [69]). Combined with the characteristics of rounded–subrounded zircons and coarse-grained sandstone, it is suggested that this age population, coupled with the ~1400 Ma cluster, might have deposited in SKT older sandstones after being transported a long distance and redeposited in the Malieziken Group. In addition, the age spectra with a predominant age peak of ~1100 Ma from the Malieziken Group are similar to those from East Sumatra, Lhasa, and Western Australia (Figure 9), implying the SKT and these blocks have undergone a similar event, which implies a close affinity between SKT and Western Australia.

The Tarim basin and SKT was separated by the Proto-Tethys Ocean during the Cambrian and Ordovician, so that there is a lack of detritus sediment supply from the Tarim to the SKT. The age spectra of Malieziken Group are not similar to the North Tarim and South Tarim, implying detritus is rarely sourced from STT or NTT.

In summary, the detritus of the Malieziken Group is mainly sourced from SKT itself, such as the underlying Sangzhotage Group, Kudi ophiolite (subduction of Proto-Tethys Ocean), Sailajiazitage Group, and redeposited materials from Western Australia, and other adjacent terranes in East Gondwana, but rarely from the Tarim Basin.

5.3. Possible Position of Tarim Block in Gondwana

The position of the Tarim block in Gondwana has been disputed by several studies, including in Western Australia [13–16,28], North India [10–12], Sibumasu [7,81,82] and Saudi Arabia–Iran [9,83,84]. To position the Tarim block in East Gondwana, detrital zircons U–Pb ages from Malieziken Group in SKT are compiled and compared with detrital zircons age spectra of potential adjacent blocks (Figure 9).

The Malieziken Group detrital zircons are characterized by two main peaks at ~490 Ma and ~1100 Ma, and three subordinate peaks at ~880 Ma, ~1400 Ma, and ~1650 Ma (Figure 9a). The detrital zircon age spectra from the Malieziken Group are very similar to those from East Sumatra (Figure 9e), implying a close affinity between Tarim block with East Sumatra.

The presence of ~1100 Ma predominant peak from Malieziken Group indicates that the SKT underwent a similar tectonic event with Western Australia (Figure 9g) but not North India (Figure 9h). East Sumatra and Lhasa also show the predominant peak at ~1100 Ma (Figure 9e,f), and the two blocks are generally considered to be situated at the northwestern margin of Western Australia (Figure 10, [14,72,85,86]). The peaks ~490 Ma recorded the double-sided subduction of the Proto-Tethys Ocean and the collision of SKT and NKT (Tarim) [35,58,75]. Furthermore, the absent ~1400 Ma and ~1650 Ma peak of the QT04-1 correlated well with the Albany–Fraser orogen Paleoproterozoic strata (Figure 7, [69], see Section 5.2), suggesting part of the detritus of Malieziken Group might be from Western Australia.

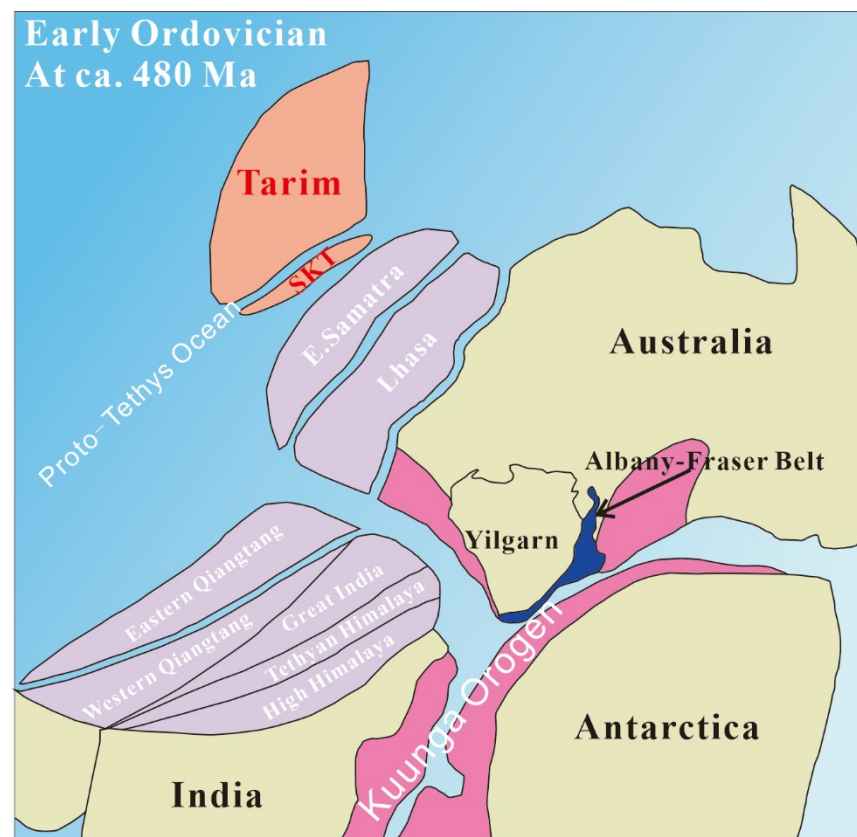


Figure 10. Possible paleoposition of Tarim in East Gondwana in the Ordovician, Modified from [85]. The position of East Sumatra is from [72,86].

The inference that Tarim block has a close affinity with East Sumatra, Lhasa, and Western Australia is also supported by similar fossil assemblages and paleoenvironment [7,82]. We proposed that the Tarim block occupied a position outboard East Sumatra, close to Lhasa and the northwest margin of Western Australia (Figure 10).

6. Conclusions

We report U-Pb ages of 316 detrital zircons from two sandstone samples and a limestone sample from the Malieziken Group, South Kunlun Terrane. Most zircon ages ranged from 450 Ma to 2800 Ma. Zircon U-Pb ages from Malieziken Group led us to draw the following conclusions:

1. Based on the maximum depositional age analysis, in combination with previous studies, we proposed that the Qiate formation was deposited in Early Ordovician and the Kandilike Formation was deposited in Early–Middle Ordovician.
2. The provenance of the Middle Ordovician Malieziken Group in the SKT, is constrained by comparing age spectra with adjacent igneous and metamorphic events. The

Malieziken Group strata were possibly sourced from SKT, such as the underlying Sangzhotage Group, Kudi ophiolite (subduction of Proto-Tethys Ocean), Sailajiazitage Group, and redeposited materials from Western Australia, and other adjacent terranes in East Gondwana, but rarely from the Tarim Basin, due to the Proto-Tethys Ocean between SKT and Tarim.

- Well-comparable zircon age spectra and inferred recycled detrital zircon from Western Australia suggest the SKT and Tarim block has a close linkage with East Sumatra, Lhasa, and Western Australia in East Gondwana during the Ordovician.

Supplementary Materials: The following supporting information can be downloaded at: <https://www.mdpi.com/article/10.3390/min13010042/s1>, Table S1: LA-ICP-MS in situ spot analysis of U-Pb isotopes in the Malieziken Group.

Author Contributions: Conceptualization, Z.C. and Z.G.; methodology, Z.C. and L.Z.; formal analysis, Z.C.; investigation, Z.C. and J.W.; writing—original draft, Z.C.; visualization, Z.C.; resources, Z.G. and J.W.; supervision, Z.G.; project administration, Z.G.; funding acquisition, Z.G.; writing—review and editing, L.Z., T.F. and D.W.; data curation, J.W. All authors have read and agreed to the published version of the manuscript.

Funding: This research was funded by National Natural Science Foundation of China grant number 41972130.

Acknowledgments: We thank Zhihong Kang for his help in field work, and Ningyuan Qi, Xiang Liu, Qi Wang, and Kai Xu for their help in the experiment of zircon U-Pb age analysis. Constructive suggestions by Jiajun Chen are gratefully acknowledged.

Conflicts of Interest: The authors declare no conflict of interest.

References

- Stampfli, G.M.; Borel, G.D. A plate tectonic model for the Paleozoic and Mesozoic constrained by dynamic plate boundaries and restored synthetic oceanic isochrones. *Earth Planet. Sci. Lett.* **2002**, *196*, 17–33. [\[CrossRef\]](#)
- Veevers, J.J. Gondwanaland from 650–500 Ma assembly through 320 Ma merger in Pangea to 185–100 Ma breakup: Supercontinental tectonics via stratigraphy and radiometric dating. *Earth-Sci. Rev.* **2004**, *68*, 1–132. [\[CrossRef\]](#)
- Cocks, L.R.M.; Torsvik, T.H. The dynamic evolution of the Palaeozoic geography of eastern Asia. *Earth-Sci. Rev.* **2013**, *117*, 40–79. [\[CrossRef\]](#)
- Burrett, C.; Stait, B. China and Southeast Asia as part of the Tethyan margin of Cambro-Ordovician Gondwanaland. In *Shallow Tethys 2*; McKenzie, K., Ed.; Balkema: Rotterdam, The Netherlands, 1987; pp. 65–77.
- Burrett, C.; Long, J.; Stait, B. Early–Middle Palaeozoic biogeography of Asian terranes derived from Gondwana. *Geol. Soc. Lond. Mem.* **1990**, *12*, 163–174. [\[CrossRef\]](#)
- Metcalfe, I. Palaeozoic-Mesozoic history of SE Asia. In *The SE Asian Gateway: History and Tectonics of the Australia–Asia Collision*; Hall, R., Cottam, M.A., Wilson, M.E.J., Eds.; Geological Society, Special Publications: London, UK, 2011; Volume 355, pp. 7–35.
- Fang, X.; Burrett, C.; Li, W.; Zhang Yunbai Zhang Yuandong Chen, T.; Wu, X. Dynamic variation of Middle to Late Ordovician cephalopod provincialism in the northeastern peri-Gondwana region and its implications. *Palaeogeogr. Palaeoclimatol. Palaeoecol.* **2019**, *521*, 127–137. [\[CrossRef\]](#)
- Li, Z.X.; Evans, D.A.; Halverson, G.P. Neoproterozoic glaciations in a revised global palaeogeography from the breakup of Rodinia to the assembly of Gondwanaland. *Sediment. Geol.* **2013**, *294*, 219–232. [\[CrossRef\]](#)
- Zhao, G.; Wang, Y.; Huang, B.; Dong, Y.; Li, S.; Zhang, G.; Yu, S. Geological reconstructions of the East Asian blocks: From the breakup of Rodinia to the assembly of Pangea. *Earth-Sci. Rev.* **2018**, *186*, 262–286. [\[CrossRef\]](#)
- Liu, Q.; Zhao, G.; Li, J.; Yao, J.; Han, Y.; Wang, P.; Tsunogae, T. Detrital Zircon U-Pb-Hf Isotopes of Middle Neoproterozoic Sedimentary Rocks in the Altyn Tagli Orogen, Southeastern Tarim: Insights for a Tarim-South China-North India Connection in the Periphery of Rodinia. *Lithosphere* **2020**, *2020*, 8895888. [\[CrossRef\]](#)
- Wang, P.; Zhao, G.; Cawood, P.A.; Han, Y.; Yu, S.; Liu, Q.; Yao, J.; Zhang, D. South Tarim tied to north India on the periphery of Rodinia and Gondwana and implications for the evolution of two supercontinents. *Geology* **2022**, *50*, 131–136. [\[CrossRef\]](#)
- Wang, P.; Zhao, G.; Han, Y.; Liu, Q.; Yao, J.; Yu, S. Position of the Tarim Craton in Gondwana: Constraints from Neoproterozoic to early Paleozoic strata in south Tarim, NW China. *Tectonophysics* **2021a**, *803*, 228741. [\[CrossRef\]](#)
- Li, Z.X.; Bogdanova, S.V.; Collins, A.S.; Davidson, A.; De Waele, B.; Ernst, R.E.; Fitzsimons, I.C.W.; Fuck, R.A.; Gladkochub, D.P.; Jacobs, J.; et al. Assembly, configuration, and break-up history of Rodinia: A synthesis. *Precambrian Res.* **2008**, *160*, 179–210. [\[CrossRef\]](#)
- Metcalfe, I. Gondwana dispersion and Asian accretion: Tectonic and palaeogeographic evolution of eastern Tethys. *J. Asian Earth Sci.* **2013**, *66*, 1–33. [\[CrossRef\]](#)

15. Powell, C.M.; Pisarevsky, S.A. Late Neoproterozoic assembly of East Gondwana. *Geology* **2002**, *30*, 3–6. [\[CrossRef\]](#)
16. Zhao, P.; Chen, Y.; Zhan, S.; Xu, B.; Faure, M. The Apparent Polar Wander Path of the Tarim block (NW China) since the Neoproterozoic and its implications for a long-term Tarim-Australia connection. *Precambrian Res.* **2014**, *242*, 39–57. [\[CrossRef\]](#)
17. Mattern, F.; Schneider, W. Suturing of the Proto- and Paleo-Tethys oceans in the western Kunlun (Xinjiang, China). *J. Asian Earth Sci.* **2000**, *18*, 637–650. [\[CrossRef\]](#)
18. Jiang, Y.H.; Jiang, S.Y.; Ling, H.F.; Zhou, X.R.; Rui, X.J.; Yang, W.Z. Petrology and geochemistry of shoshonitic plutons from the western Kunlun orogenic belt, northwestern Xinjiang, China: Implications for granitoid gneisses. *Lithos* **2002**, *63*, 165–187. [\[CrossRef\]](#)
19. Zhang, C.L.; Zou, H.B.; Ye, X.T.; Chen, X.Y. Tectonic evolution of the West Kunlun Orogenic Belt along the northern margin of the Tibetan Plateau: Implications for the assembly of the Tarim terrane to Gondwana. *Geosci. Front.* **2019c**, *10*, 973–988. [\[CrossRef\]](#)
20. Xinjiang Bureau of Geology and Mineral Resources. *Regional Geology of the Xinjiang Uygur Autonomous Region*; Geological Publishing House: Beijing, China, 1993; pp. 17–45. (In Chinese)
21. Liu, D.Y.; Zhang, Z.X.; Di, Q.L. Middle Ordovician Brachiopods from Kunlun-Altyn area. *Acta Paleontol. Sin.* **1984**, *23*, 155–169. (In Chinese)
22. Yin, H.M.; Xia, F.S. Discovery of *Batostoma* in Lower Malieziken Group, Ruoqiang area, Xinjiang. *Acta Micropalaeontologica Sin.* **1986**, *3*, 435–440. (In Chinese)
23. Wang, P. Discovery of Ordovician graptolite bearing strata in Kandilike area, West Kunlun. *J. Stratigr.* **2001**, *25*, 123–124. (In Chinese)
24. Qian, Y.X.; Wang, L.; Kang, Z.H.; Chen, Y.; Jia, C.S.; Tian, M.; Zhang, Y.D. Detrital zircon Chronology research of Ordovician Malieziken Group, Southwestern Tarim. *Xinjiang Geol.* **2018**, *36*, 30–37. (In Chinese)
25. Dickinson, W.R.; Gehrels, G.E. Use of U-Pb ages of detrital zircons to infer maximum depositional ages of strata: A test against a Colorado Plateau Mesozoic database. *Earth Planet. Sci. Lett.* **2009**, *288*, 115–125. [\[CrossRef\]](#)
26. Tucker, R.T.; Roberts, E.M.; Hu, Y.; Kemp, A.I.S.; Salisbury, S.W. Detrital zircon age constraints for the Winton Formation, Queensland: Contextualizing Australia's Late Cretaceous dinosaur faunas. *Gondwana Res.* **2013**, *24*, 767–779. [\[CrossRef\]](#)
27. Cawood, P.A.; Wang, Y.; Xu, Y.; Zhao, G. Locating South China in Rodinia and Gondwana: A fragment of greater India lithosphere? *Geology* **2013**, *41*, 903–906. [\[CrossRef\]](#)
28. Han, Y.; Zhao, G.; Sun, M.; Eizenhöfer, P.R.; Hou, W.; Zhang, X.; Liu, D.; Wang, B.; Zhang, G. Paleozoic accretionary orogenesis in the Paleo-Asian Ocean: Insights from detrital zircons from Silurian to Carboniferous strata at the northwestern margin of the Tarim craton. *Tectonics* **2015**, *34*, 334–351. [\[CrossRef\]](#)
29. Morag, N.; Avigad, D.; Gerdes, A.; Belousova, E.; Harlavan, Y. Detrital zircon Hf isotopic composition indicates long-distance transport of North Gondwana Cambrian-Ordovician sandstones. *Geology* **2011**, *39*, 955–958. [\[CrossRef\]](#)
30. Myrow, P.M.; Hughes, N.C.; Goodge, J.W.; Fanning, C.M.; Williams, I.S.; Peng, S.; Bhargava, O.N.; Parcha, S.K.; Pogue, K.R. Extraordinary transport and mixing of sediment across Himalayan central Gondwana during the Cambrian-Ordovician. *Geol. Soc. Am. Bull.* **2010**, *122*, 1660–1670. [\[CrossRef\]](#)
31. Zhang, C.L.; Zou, H.B.; Li, H.K.; Wang, H.Y. Tectonic framework and evolution of the Tarim Block in NW China. *Gondwana Res.* **2013**, *23*, 1306–1315. [\[CrossRef\]](#)
32. Yang, H.; Wu, G.; Kusky, T.M.; Chen, Y.; Xiao, Y. Paleoproterozoic assembly of the North and South Tarim terranes: New insights from deep seismic profiles and Precambrian granite cores. *Precambrian Res.* **2018**, *305*, 151–165. [\[CrossRef\]](#)
33. Wen, B.; Evans, D.A.; Wang, C.; Li, Y.X.; Jing, X. A positive test for the Greater Tarim Block at the heart of Rodinia: Mega-dextral suturing of supercontinent assembly. *Geology* **2018**, *46*, 687–690. [\[CrossRef\]](#)
34. Zhao, P.; He, J.; Deng, C.; Chen, Y.; Mitchell, R.N. Early Neoproterozoic (870–820 Ma) amalgamation of the Tarim craton (northwestern China) and the final assembly of Rodinia. *Geology* **2021**, *49*, 1277–1282. [\[CrossRef\]](#)
35. Zhu, G.Y.; Chen, Z.Y.; Chen, W.Y.; Yan, H.H.; Zhang, P.H. Revisiting to the Neoproterozoic tectonic evolution of the Tarim Block, NW China. *Precambrian Res.* **2021**, *352*, 106013. [\[CrossRef\]](#)
36. Hu, J.; Wang, H.; Wang, M. Provenance and tectonic setting of siliciclastic rocks associated with the Neoproterozoic Dahongliutan BIF: Implications for the Precambrian crustal evolution of the Western Kunlun orogenic belt, NW China. *J. Asian Earth Sci.* **2017**, *147*, 95–115. [\[CrossRef\]](#)
37. Yin, J.; Xiao, W.; Sun, M.; Chen, W.; Yuan, C.; Zhang, Y.; Wang, T.; Du, Q.; Wang, X.; Xia, X. Petrogenesis of Early Cambrian granitoids in the western Kunlun orogenic belt, Northwest Tibet: Insight into early stage subduction of the Proto-Tethys Ocean. *Bull. Geol. Soc. Am.* **2020**, *132*, 2221–2240. [\[CrossRef\]](#)
38. Pan, G.T.; Zhu, D.C.; Wang, L.Q.; Liao, Z.L.; Geng, Q.R.; Jiang, X.S. Banggong Lake- Nu River suture zone-the northern boundary of Gondwanaland: Evidence from geology and geophysics. *Earth Sci. Front.* **2004**, *11*, 371–382. (In Chinese)
39. Zhang, C.L.; Lu, S.N.; Yu, H.F.; Ye, H.M. Tectonic evolution of the Western Kunlun orogenic belt in the northern margin of the Tibetan Plateau: Evidence from SHRIMP and LA-ICP-MS Zircon dating. *Sci. China Ser. D:Earth Sci.* **2007**, *37*, 145–154. (In Chinese)
40. Hu, J.; Wang, H.; Huang, C.Y.; Tong, L.X.; Mu, S.L.; Qiu, Z.W. Geological characteristics and age of the Dahongliutan Fe-ore deposit in the Western Kunlun orogenic belt, Xinjiang, northwestern China. *J. Asian Earth Sci.* **2016**, *116*, 1–25. [\[CrossRef\]](#)
41. Zhang, C.L.; Ye, X.T.; Ernst, R.E.; Zhong, Y.; Zhang, J.; Li, H.K.; Long, X.P. Revisiting the Precambrian evolution of the Southwestern Tarim terrane: Implications for its role in Precambrian supercontinents. *Precambrian Res.* **2019b**, *324*, 18–31. [\[CrossRef\]](#)

42. Xiao, W.J.; Windley, B.F.; Hao, J.; Li, J.L. Arc-ophiolite obduction in the Western Kunlun Range (China): Implications for the Paleozoic evolution of central Asia. *J. Geol. Soc.* **2002**, *159*, 517–528. [[CrossRef](#)]
43. Xiao, W.J.; Han, F.L.; Windley, B.F.; Yuan, C.; Zhou, L.; Li, J.L. Multiple accretionary orogenesis and episodic growth of continents: Insights from the Western Kunlun Range, central Asia. *Int. Geol. Rev.* **2003**, *45*, 303–328. [[CrossRef](#)]
44. Jiang, Y.H.; Jia, R.Y.; Liu, Z.; Liao, S.Y.; Zhao, P.; Zhou, P. Origin of Middle Triassic high-K calc-alkaline granitoids and their potassic microgranular enclaves from the western Kunlun orogen, northwest China: A record of the closure of Paleo-Tethys. *Lithos* **2013**, *156–159*, 13–30. [[CrossRef](#)]
45. Dong, Y.G.; Guo, K.Y.; Xiao, H.L.; Zhang, C.L.; Zhao, Y. Ore-forming conditions and prospecting in the West Kunlun area, Xinjiang, China. *Acta Geol. Sin.* **2004**, *78*, 345–351.
46. Pirajno, F. *The Geology and Tectonic Settings of China's Mineral Deposits*; Springer: Berlin, Germany, 2013; pp. 1–671.
47. Wang, C.; Wang, Y.H.; Liu, L.; He, S.P.; Li, R.S.; Li, M.; Yang, W.Q.; Cao, Y.T.; Meert, J.G.; Shi, C. The Paleoproterozoic magmatic-metamorphic events and cover sediments of the Tiekelik Belt and their tectonic implications for the southern margin of the Tarim Craton, northwestern China. *Precambrian Res.* **2014**, *254*, 210–225. [[CrossRef](#)]
48. Zhang, C.L.; Ye, X.T.; Zou, H.B.; Chen, X.Y. Neoproterozoic sedimentary basin evolution in southwestern Tarim, NW China: New evidence from field observations, detrital zircon U-Pb ages and Hf isotope compositions. *Precambrian Res.* **2016**, *280*, 31–45. [[CrossRef](#)]
49. Ye, X.T.; Zhang, C.L.; Santosh, M.; Zhang, J.; Fan, X.K.; Zhang, J.J. Growth and evolution of Precambrian continental crust in the southwestern Tarim terrane: New evidence from the ca. 1.4 Ga A-type granites and Paleoproterozoic intrusive complex. *Precambrian Res.* **2016**, *275*, 18–34. [[CrossRef](#)]
50. Gaetani, M.; Gosso, G.; Pognante, U. A geological transect from Kunlun to Karakorum (Sinkiang, China): The western termination of the Tibetan Plateau. Preliminary note. *Terra Nova* **1990**, *2*, 23–30. [[CrossRef](#)]
51. Yuan, C.; Sun, M.; Yang, J.T.; Zhou, H.; Zhou, M.F. Akaz greenschist, West Kunlun: Within-plate basalt contaminated by continental crust origin of the Akaz greenschist (metabasalt), West Kunlun: Accreted seamount or continental rift basalt? *Acta Geol. Sin.* **2005**, *21*, 65–67. (In Chinese)
52. Yuan, C.; Sun, M.; Zhou, M.F.; Zhou, H.; Xiao, W.J.; Li, J.L. Tectonic evolution of the West Kunlun: Geochronologic and geochemical constraints from Kudi granitoids. *Int. Geol. Rev.* **2002**, *44*, 653–669. [[CrossRef](#)]
53. Cui, J.T.; Wang, J.C.; Bian, X.W.; Zhu, H.P.; Luo, Q.Z.; Yang, K.J.; Wang, M.C. Zircon SHRIMP U-Pb dating of early Paleozoic granite in the Menggubao-Pushou area on the northern side of Kangxiwar, West Kunlun. *Geol. Bull. China* **2007**, *26*, 710–719. (In Chinese)
54. Jiang, C.F.; Yang, J.S.; Feng, B.G.; Zhu, Z.Z.; Zhao, M.; Cai, Y.C. *The Opening–Closing Tectonics of Kunlun Terrane*; Geological Publishing House: Beijing, China, 1992; 58p. (In Chinese)
55. He, B.; Jiao, C.; Xu, Z.; Cai, Z.; Zhang, J.; Liu, S.; Li, H.; Chen, W.; Yu, Z. The paleotectonic and paleogeography reconstructions of the Tarim Basin and its adjacent areas (NW China) during the late Early and Middle Paleozoic. *Gondwana Res.* **2016**, *30*, 191–206. [[CrossRef](#)]
56. Zhang, Q.; Wu, Z.; Chen, X.; Zhou, Q.; Shen, N. Proto-Tethys oceanic slab break-off: Insights from early Paleozoic magmatic diversity in the West Kunlun Orogen, NW Tibetan Plateau. *Lithos* **2019e**, *346–347*, 105147. [[CrossRef](#)]
57. Xiao, W.J.; Windley, B.F.; Liu, D.Y.; Jian, P.; Liu, C.Z.; Yuan, C.; Sun, M. Accretionary tectonics of the Western Kunlun Orogen, China: A Paleozoic–early Mesozoic, long-lived active continental margin with implications for the growth of Southern Eurasia. *J. Geol.* **2005**, *113*, 687–705. [[CrossRef](#)]
58. Wang, P.; Zhao, G.; Han, Y.; Liu, Q.; Yao, J.; Yu, S.; Li, J. Timing of the final closure of the Proto-Tethys Ocean: Constraints from provenance of early Paleozoic sedimentary rocks in West Kunlun, NW China. *Gondwana Res.* **2020**, *84*, 151–162. [[CrossRef](#)]
59. Wang, P.; Zhao, G.; Liu, Q.; Han, Y.; Zhang, Y.; Yao, J.; Yu, S. Slab-controlled progressive evolution of the Kudi back-arc ophiolite in response to the rollback of the Proto-Tethys oceanic slab, in Western Kunlun, NW Tibetan Plateau. *Lithos* **2021b**, *380–381*, 105877. [[CrossRef](#)]
60. Zhu, G.Y.; Ren, R.; Chen, F.R.; Li, T.T.; Chen, Y.Q. Neoproterozoic rift basins and their control on the development of hydrocarbon source rocks in the Tarim Basin, NW China. *J. Asian Earth Sci.* **2017**, *150*, 63–72. [[CrossRef](#)]
61. Gao, Z.; Fan, T. Carbonate platform-margin architecture and its influence on Cambrian-Ordovician reef-shoal development, Tarim Basin, NW China. *Mar. Pet. Geol.* **2015**, *68*, 291–306. [[CrossRef](#)]
62. Gao, Z.; Fan, T. An Early Paleozoic Inter-Platform Shelf in the Southwest of Tarim Basin, NW China and its Significance for Petroleum Exploration. *Resour. Geol.* **2014**, *64*, 346–366.
63. Zhang, L.L.; Zhu, D.C.; Wang, Q.; Zhao, Z.D.; Liu, D.; Xie, J.C. Late Cretaceous volcanic rocks in the Sangri area, southern Lhasa Terrane, Tibet: Evidence for oceanic ridge subduction. *Lithos* **2019d**, *326–327*, 144–157. [[CrossRef](#)]
64. Jackson, S.E.; Pearson, N.J.; Griffin, W.L.; Belousova, E.A. The application of laser ablation-inductively coupled plasma-mass spectrometry to in situ U–Pb zircon geochronology. *Chem. Geol.* **2004**, *211*, 47–69. [[CrossRef](#)]
65. Griffin, W.L.; Belousova, E.A.; Shee, S.R.; Pearson, N.J.; O'Reilly, S.Y. Archean crustal evolution in the northern Yilgarn craton: U–Pb and Hf-isotope evidence from detrital zircons. *Precambrian Res.* **2004**, *131*, 231–282. [[CrossRef](#)]
66. Ludwig, K.R. (Ed.) *Isoplot/Ex (rev. 3.75): A Geochronological Toolkit for Microsoft Excel*; Berkeley Geochronology Center, Special publication: Berkeley, CA, USA, 2012; pp. 1–75.
67. Corfu, F.; Hanchar, J.M.; Hoskin, P.W.; Kinny, P. Atlas of zircon textures. *Rev. Mineral. Geochem.* **2003**, *53*, 469–500. [[CrossRef](#)]

68. Cawood, P.A.; Hawkesworth, C.J.; Dhuime, B. Detrital zircon record and tectonic setting. *Geology* **2012**, *40*, 875–878. [[CrossRef](#)]
69. Spaggiari, C.V.; Kirkland, C.L.; Smithies, R.H.; Wingate, M.T.D.; Belousova, E.A. Transformation of an Archean craton margin during Proterozoic basin formation and magmatism: The Albany-Fraser Orogen, Western Australia. *Precambrian Res.* **2015**, *266*, 440–466. [[CrossRef](#)]
70. Dong, S.; Li, Z.; Xu, J.; Gao, J.; Guo, C. Detrital zircon U–Pb geochronology and Hf isotopic compositions of Middle–Upper Ordovician sandstones from the Quruqtagh area, eastern Tarim Basin: Implications for sedimentary provenance and tectonic evolution. *Chin. Sci. Bull.* **2014**, *59*, 1002–1012. [[CrossRef](#)]
71. Dong, S.; Li, Z.; Jiang, L. The early Paleozoic sedimentary-tectonic evolution of the circum-Mangar areas, Tarim block, NW China: Constraints from integrated detrital records. *Tectonophysics* **2016**, *682*, 17–34. [[CrossRef](#)]
72. Zhang, X.; Chung, S.L.; Lai, Y.M.; Ghani, A.A.; Murtadha, S.; Lee, H.Y.; Hsu, C.C. Detrital Zircons Dismember Sibumasu in East Gondwana. *J. Geophys. Res. Solid Earth* **2018**, *123*, 6098–6110. [[CrossRef](#)]
73. Chen, L.R.; Xu, W.C.; Zhang, H.F.; Guo, J.L.; Luo, B.J. The influence of tectonic and climatic factors on detrital zircon U[²³⁸]Pb age population of Paleozoic metasedimentary rocks in the Lhasa terrane. *Lithos* **2022**, *418–419*, 106670. [[CrossRef](#)]
74. He, D.F.; Zhou, X.Y.; Zhang, C.J.; Yang, X.F. The proto-type basin evolution of the Ordovician in Tarim area. *Chin. Sci. Bull.* **2007**, *52*, 126–135. (In Chinese) [[CrossRef](#)]
75. Wu, K.; Zhang, L.; Jiang, X.; Chen, Y.; Guo, J.; Sun, W.; Sui, Q.; Yuan, H. Continental crust growth during the evolution of accretionary orogens: Insights from the early Paleozoic granitoids in the Western Kunlun orogen, Northwest China. *Lithos* **2021**, *398–399*, 106253. [[CrossRef](#)]
76. Li, T.F.; Zhang, J.X. Zircon LA-ICP-MS U–Pb ages of websterite and basalt in Kudi ophiolite and the implication, West Kunlun. *Acta Petrol. Sin.* **2014**, *30*, 2393–2401. (In Chinese)
77. Wang, C.M.; Tang, H.S.; Zheng, Y.; Dong, L.H.; Li, J.H.; Qu, X. Early Paleozoic magmatism and metallogeny related to Proto-Tethys subduction: Insights from volcanic rocks in the northeastern Altyn Mountains, NW China. *Gondwana Res.* **2019**, *75*, 134–153. [[CrossRef](#)]
78. Wang, C.; Zhang, J.H.; Li, M.; Li, R.S.; Peng, Y. Generation of ca. 900–870 Ma bimodal rifting volcanism along the southwestern margin of the Tarim Craton and its implications for the Tarim–North China connection in the early Neoproterozoic. *J. Asian Earth Sci.* **2015**, *113*, 610–625. [[CrossRef](#)]
79. Zhang, C.L.; Li, H.K.; Ernst, R.E.; Zhu, G.Y.; Liu, X.Q.; Zhang, J.; Zhong, Y.; Hao, X.S. A fragment of the ca. 890 Ma large igneous province (LIP) in southern Tarim, NW China: A missing link between São Francisco, Congo and North China cratons. *Precambrian Res.* **2019a**, *333*, 105428. [[CrossRef](#)]
80. Xu, Z.Q.; He, B.Z.; Zhang, C.L.; Zhang, J.X.; Wang, Z.M.; Cai, Z.H. Tectonic framework and crustal evolution of the Precambrian basement of the Tarim Block in NW China: New geochronological evidence from deep drilling samples. *Precambrian Res.* **2013**, *235*, 150–162. [[CrossRef](#)]
81. Metcalfe, I. Kyi Pyar Aung Late Tournaisian conodonts from the Taungnyo Group near Loi Kaw, Myanmar (Burma): Implications for Shan Plateau stratigraphy and evolution of the Gondwana-derived Sibumasu Terrane. *Gondwana Res.* **2014**, *26*, 1159–1172. [[CrossRef](#)]
82. Burrett, C.; Zaw, K.; Meffre, S.; Lai, C.K.; Khositantont, S.; Chaodumrong, P.; Udchachon, M.; Ekins, S.; Halpin, J. The configuration of Greater Gondwana-Evidence from LA ICPMS, U–Pb geochronology of detrital zircons from the Palaeozoic and Mesozoic of Southeast Asia and China. *Gondwana Res.* **2014**, *26*, 31–51. [[CrossRef](#)]
83. Bian, Q.T.; Li, D.H.; Pospelov, I.; Yin, L.M.; Li, H.S.; Zhao, D.S. Age, geochemistry and tectonic setting of Buqingshan ophiolites, North Qinghai-Tibet Plateau, China. *J. Asian Earth Sci.* **2004**, *234*, 577–596.
84. Huang, B.; Piper, J.D.; Sun, L.; Zhao, Q. New paleomagnetic results for Ordovician and Silurian rocks of the Tarim Block, Northwest China and their paleogeographic implications. *Tectonophysics* **2019**, *755*, 91–108.
85. Zhu, D.C.; Zhao, Z.D.; Niu, Y.; Dilek, Y.; Mo, X.X. Lhasa terrane in Southern Tibet came from Australia. *Geology* **2011**, *39*, 727–730. [[CrossRef](#)]
86. Song, Y.; Su, L.; Dong, J.; Song, S.; Allen, M.B.; Wang, C.; Hu, X. Detrital zircons from Late Paleozoic to Triassic sedimentary rocks of the Gongshan-Baoshan Block, SE Tibet: Implications for episodic crustal growth of Eastern Gondwana. *J. Asian Earth Sci.* **2020**, *188*, 104106.

Disclaimer/Publisher’s Note: The statements, opinions and data contained in all publications are solely those of the individual author(s) and contributor(s) and not of MDPI and/or the editor(s). MDPI and/or the editor(s) disclaim responsibility for any injury to people or property resulting from any ideas, methods, instructions or products referred to in the content.